center frequency of the coupler. The exact role that each of these elements plays in the final, fully compensated configuration is difficult to assess, and no attempt at a detailed analysis has been made.

In summary, a solution to the problem of anisotropy drift in a YIG single crystal gyromagnetic coupler has been achieved through the appropriate orientation of the YIG coupling element. A solution to the external source of instability has been achieved through the use of a magnetic shunt of Carpenter Temperature Compensator. The end product is a well shielded gyromagnetic coupler, tunable from 5.4 to 5.7 Gc, free from anisotropy drift affects with up to 1 watt average power input, and temperature stabilized to less than ±2 Mc through an ambient change from −20°F to 150°F.

ACKNOWLEDGMENT

The authors wish to thank Drs. G. P. Rodrigue and J. E. Pippin of Sperry Microwave Electronics Company, Research Section, for many valuable suggestions.

J. CLARK
J. BROWN
D. E. TRIBBY
Advance Microwave Techniques Dept.
Sperry Microwave Electronics Co.
Clearwater, Fla.

An S-Band Wide-Band Degenerate Parametric Amplifier*

This communication reports some experimental results for an S-band wide-band degenerate parametric amplifier designed with a method earlier described by the author.[1]

We represent the varactor by a nonlinear capacitance in series with a loss resistance R and an inductance L_s and write the pumped capacitance as

$$C = C_d[1 + 2\alpha \cos \omega_p t]. \quad (1)$$

Then the signal voltage gain G of a degenerate circulator operated amplifier can be written as

$$\begin{cases} |G| = \dfrac{1 + |\rho|^2}{2|\rho|} \\ \rho = \dfrac{Z_s - Z_d}{Z_s + Z_d} \end{cases} \quad (2)$$

Z_s is the signal circuit impedance, including varactor reactances, as seen from the varactor end. Z_d is a modified signal-idler coupling impedance

$$\begin{cases} Z_{d0} = \dfrac{\alpha}{\omega_{s0}(1 - \alpha^2)C_d} \\ Z_d = \sqrt{Z_{d0}^2 + \dfrac{R^2}{G_0^2 - 1}} - R\dfrac{G_0}{\sqrt{G_0^2 - 1}} \end{cases} \quad (3)$$

* Received May 24, 1963.

[1] B. T. Henoch, "A new method for designing wide-band parametric amplifiers," IEEE TRANS. ON MICROWAVE THEORY AND TECHNIQUES, vol. MTT-11, pp. 62–72; January, 1963.

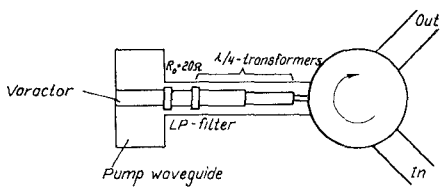

Fig. 1—Configuration of a single-tuned amplifier.

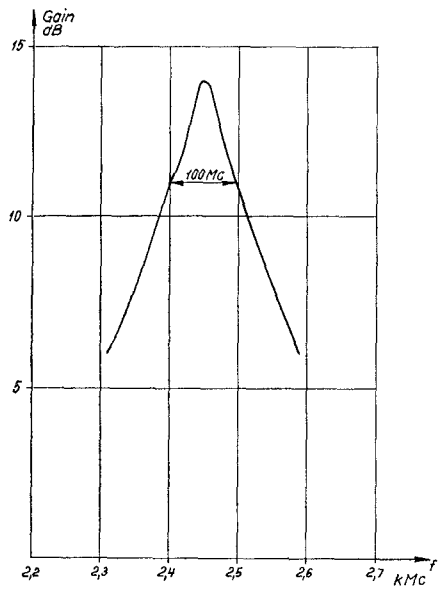

Fig. 2—Double sideband gain as a function of frequency for the single-tuned amplifier.

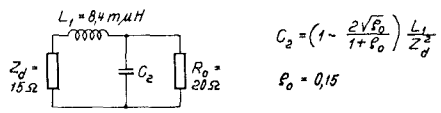

Fig. 3—Low-pass equivalent of the matching circuit.

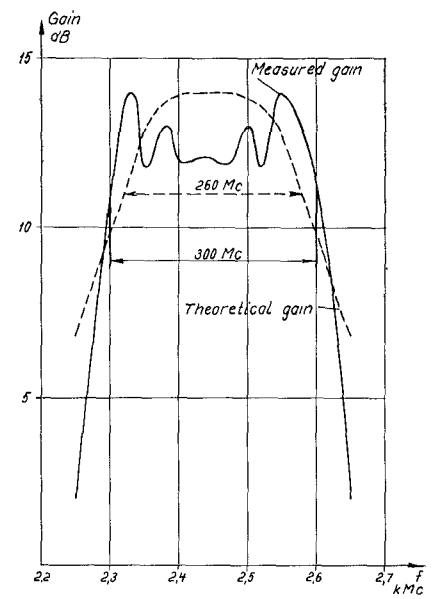

Fig. 4—Double sideband gain as a function of frequency for the double-tuned amplifier.

The wide-band design problem now is reduced to a problem of matching the modified coupling impedance Z_d into the amplifier source impedance R_0.

The experimental amplifier uses a GaAs varactor with a zero-bias capacitance of 0.5 pf, cutoff frequency 100 kMc and series-resonance frequency 6 kMc. The varactor is mounted in a pump waveguide according to Fig. 1.

The signal frequency is chosen so that the waveguide inductance resonates the varactor and the amplifier source impedance R_0 is chosen to 20 Ω.

The double sideband gain is measured by using a swept frequency generator and a broad-band detector which displays the gain curve on an oscilloscope. The gain vs frequency for the single-tuned amplifier is shown in Fig. 2.

The measured gain curve corresponds to C_d=0.5 pf, Z_d=15 Ω and α=0.15. The inductance L_1 in the series resonator is L_1=8.4 mμh.

To get a double-tuned wide-band amplifier a parallel resonator is inserted between the series-tuned varactor and the amplifier source impedance R_0 and designed to match Z_d maximally flat into R_0. The low-pass equivalent of the matching circuit is shown in Fig. 3.

Practically, a low impedance section, half a wavelength long at ω_{s0}, is used as a parallel resonator. From a linear approximation around ω_{s0} the impedance Z_p of the low impedance section can be determined.

$$C_2 = \frac{1}{2}\frac{\pi}{\omega_{s0}}\left[\frac{1}{Z_p} - \frac{Z_p}{R_0^2}\right]. \quad (4)$$

This determines Z_p to 7 Ω. Plotting in a Smith Chart shows that the optimum Z_p will be somewhat lower than given by (4). Reactive parts in the source impedance R_0 might modify the length of the low impedance section.

With a low impedance section of impedance 5.5 Ω and electrical length 170° at ω_{s0} the gain curve shown in Fig. 4 is measured. The measured gain curve is compared with a theoretical gain curve obtained from the concentrated element equivalent.

Point measurements of the double sideband noise figure give noise figures of 1.5–2.0 db.

BENGT T. HENOCH
Research Institute of National Defence
Stockholm, Sweden

Phaseshift of Electromagnetic Waves Propagating Through Waveguide Junctions*

This work was activated by the lack of information in literature about the effect of an H-plane branch upon electromagnetic waves traveling through the collinear arms of the branch. Most literature about the sub-

* Received March 29, 1963; revised manuscript received April 29, 1963.

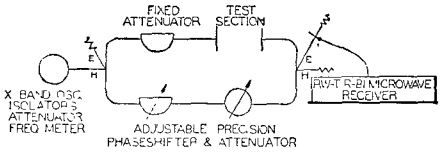

Fig. 1—The waveguide bridge circuit used to obtain the data presented in Figs. 2 and 3.

ject predicts zero degrees phaseshift across the trivial 90° branch[1,2] or clear expressions of the phaseshift are not made.[3-7]

This communication will predict the phaseshift of microwaves traveling across the collinear arms of an H-plane branch of arbitrary angle. Usually, this would be accomplished by applying complicated boundary conditions to the wave equation, however this complicated approach may not always be necessary. This communication will show a very simple method of predicting the phaseshift.

The standard waveguide bridge circuit of Fig. 1 using hybrid junctions and RG 52/U waveguide was selected as the experimental measuring device. The attenuators and phaseshifter of the bridge were precision devices. The RW-T R-B1 superheterodyne microwave receiver was used as a null detector of the bridge circuit.

A set of H-plane branches were constructed from 22.5° to 157.5° in steps of 22.5° using RG 52/U rectangular waveguide as shown in Fig. 2(a). During all tests the branch arm of the waveguide section tested was terminated with a reflectionless termination. The circles of Fig. 2(b) show the experimental results of the phaseshift across the H-plane branches from this setup. Note that the Reciprocity Theorem holds exactly; *e.g.*, the 45° branch had exactly the same phaseshift as the 135° branch.

The first attempt at explaining these experimental results was by considering the waveguide wavelength of the waves traveling across the branch to be a function of the waveguide width at that point. It is known that

$$\lambda_g(d) = \frac{\lambda_0}{\sqrt{1 + \left(\frac{\lambda_0}{2d}\right)^2}} \tag{1}$$

where d = the waveguide width where the waveguide wavelength is being considered (cm). In Fig. 2(a), ϕ = branch angle (degrees), m = tan ϕ, a = normal waveguide width (cm), $d = a + mz$ (cm), λ_0 = free-space wavelength (cm), z_1 = length of the branch section (cm), θ_1 = phaseshift across the H-plane branch (degrees), θ_2 = phaseshift across

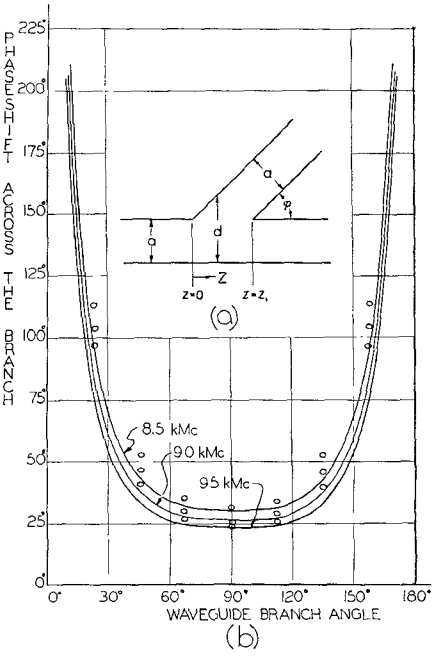

Fig. 2—(a) Waveguide H-plane junction. (b) Phaseshift across the collinear arms of H-plane waveguide branches. Circles are experimental data, curves are the theoretical phaseshifts for different frequencies; from the top, 8.5, 9.0, and 9.5 kMc.

a blank waveguide section of length z_1 (degrees), θ_T = the apparent phaseshift due to the branch in the waveguide (degrees), then

$$\theta_1 = 360 \int_0^{z_1} \frac{dz}{\lambda(d)} \tag{2}$$

$$\theta_1 = \frac{360}{m\lambda_0}\left\{\left[(a+mz_1)^2 - \frac{\lambda_0^2}{4}\right]^{1/2} - \frac{\lambda_0}{2}\cos^{-1}\left|\frac{\lambda_0}{2(a+mz_1)}\right| - \left[a^2 - \frac{\lambda_0^2}{4}\right]^{1/2} + \frac{\lambda_0}{2}\cos^{-1}\left|\frac{\lambda_0}{2a}\right|\right\} \tag{3}$$

$$\theta_2 = 360\,\frac{(z_1 - 0)}{\lambda(a)} \tag{4}$$

$$\theta_T = \theta_1 - \theta_2. \tag{5}$$

This calculation was carried out for three frequencies at all possible branch angles and found that the results broke down for angles near 90°. This was corrected by empirically keeping the waveguide width 1.170 over a distance of a, from $(z_1 - a)$ to (z_1); *e.g.*, the waveguide is considered to be $1.17a$ wide over the distance. Now we have

$$\theta_T = 360\left[\int_0^{(z_1-a)} \frac{dz}{\lambda_g(d)} - \frac{a}{\lambda(1.17a)} - \frac{(z_1 - 0)}{\lambda(a)}\right] \tag{6}$$

$$\theta_T = 360\left\{\frac{1}{m\lambda_0}\left[\langle a + m(z_1 - a)\rangle^2 - \frac{\lambda_0^2}{4}\right]^{1/2} - \frac{1}{2m}\cos^{-1}\left|\frac{\lambda_0}{2\langle a + m(z_1 - a)\rangle}\right| - \frac{1}{m\lambda_0}\left[a^2 - \frac{\lambda_0^2}{4}\right]^{1/2} + \frac{1}{2m}\cos^{-1}\left|\frac{\lambda}{2a}\right| + \frac{a}{\lambda(1.17a)} - \frac{(z_1 - 0)}{\lambda(a)}\right\}. \tag{7}$$

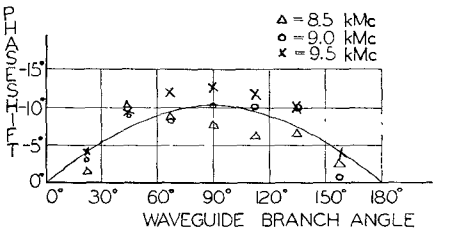

Fig. 3—Phaseshift across the collinear arms of E-plane waveguide branches. Solid curve represents the empirical equation.

This function is shown as the solid lines in Fig. 2(b) where it can be seen to predict quite satisfactorily the phaseshift across the H-plane waveguide branch.

The waveguide bridge shown in Fig. 1 was also used to measure the phaseshift across the collinear arm of a set of E-plane branches as a function of frequency and the branch angle. The experimental results are shown in Fig. 3. It was found that the phaseshift across these branches could be approximated empirically by the function,

$$\theta_T = -10.5 \sin \phi. \tag{8}$$

The solid curve in Fig. 3 represents the above empirical equation. This measured value contrasts with the phaseshift predicted for the E-plane tee by many authors.

ACKNOWLEDGMENT

The authors thank S. Krupnik, J. A. Stefancin, J. E. Billo, L. Meyer and J. Beigle for their assistance; also the Marquette University Computing Center for the use of the IBM 1620 Computer.

D. E. SCHUMACHER
K. ISHII
Dept. of Elec. Eng.
Marquette University
Milwaukee, Wis.

A New High-Power Variable Attenuator*

This communication describes a design for a variable attenuator which can operate at very high peak and average power levels propagating in any chosen mode in a single or a multimode waveguide. This attenuator offers the desirable characteristics of dissipating energy in external loads rather than within the internal structure and utilizes only one coupling mechanism. The device consists of a coupled wave structure between two modes in adjacent primary and secondary waveguides, and a suitable mechanism for varying the phase constant of the secondary waveguide.

Miller[1] has shown that, when a dis-

[1] G. C. Southworth, "Principles and Applications of Waveguide Transmission," D. Van Nostrand Co., Inc., Princeton, N. J.; 1950.
[2] H. J. Reich, P. F. Ordung, H. L. Krauss, and J. G. Skalnik, "Microwave Theory and Techniques," D. Van Nostand Co., Inc., Princeton, N. J.; 1953.
[3] H. A. Atwater, "Introduction to Microwave Theory," McGraw-Hill Book Co., Inc., New York, N. Y.; 1962.
[4] C. G. Montgomery, R. H. Dicke, and E. M. Purcell, "Principles of Microwave Circuits," McGraw-Hill Book Co., Inc., New York, N. Y.; 1948.
[5] N. Marcuvitz, "Waveguide Handbook," McGraw-Hill Book Co., Inc., New York, N. Y.; 1951.
[6] R. G. Brown, R. A. Sharpe, and W. L. Hughes, "Line, Waves and Antennas," Ronald Press Co., New York, N. Y.; 1961.
[7] T. Moreno, "Microwave Transmission Design Data," Dover Publications, New York, N. Y.; 1948.

* Received May 13, 1963. This work has been sponsored by the Wright Air Development Division under Contract No. AF33(616)6517.
[1] S. E. Miller, "Coupled wave theory and waveguide applications," *Bell Sys. Tech. J.*, vol. 33, pp. 661–719; May, 1954.